ISSN 1070-3284, Russian Journal of Coordination Chemistry, 2018, Vol. 44, No. 5, pp. 359–364. © Pleiades Publishing, Ltd., 2018

Synthesis and Characterization of a Novel Lanthanide Complex with Photoluminescent and Semiconductive Properties[1]

Z. G. Luo[a] and W. T. Chen[a, b, *]

[a] *Institute of Applied Chemistry, School of Chemistry and Chemical Engineering, Jiangxi Province Key Laboratory of Coordination Chemistry, Jinggangshan University, Ji'an, Jiangxi, 343009 P.R. China*

[b] *State Key Laboratory of Structural Chemistry, Fujian Institute of Research on the Structure of Matter, Chinese Academy of Sciences, Fuzhou, Fujian, 350002 P.R. China*

**e-mail: wtchen_2000@aliyun.com*

Received August 28, 2017

Abstract—A novel lanthanide complex $[La(2,5\text{-}PA)(2,5\text{-}HPA)(H_2O)_2]_n \cdot nH_2O$ (**I**) ($2,5\text{-}H_2PA$ = 2,5-pyridinedicarboxylic acid) was synthesized by a hydrothermal reaction and structurally characterized by single-crystal X-ray diffraction (CIF file CCDC no. 1570808). Complex **I** is characteristic of a two-dimensional (2D) layered structure with the La^{3+} ion coordinating with seven oxygen atoms and two nitrogen atoms to yield a slightly distorted monocapped square antiprism. The $[La(2,5\text{-}PA)(2,5\text{-}HPA)(H_2O)_2]_n$ layers and lattice water molecules interlink together through hydrogen bonding interactions to give a three-dimensional (3D) supramolecular framework. Photoluminescence measurements under room temperature with solid-state samples show that it displays an emission in the green region of the light spectrum. Solid-state UV-Vis spectrum conducted with solid-state samples reveals the existence of a wide optical band gap of 3.57 eV.

Keywords: crystal, lanthanide, photoluminescence, semiconductor, pyridinedicarboxylic acid

DOI: 10.1134/S1070328418050068

INTRODUCTION

Lanthanide complexes can generally show interesting photoluminescence, optical, magnetic, electronic, and chemical properties because of the 4*f* electrons of the lanthanide ions. In recent years, lanthanide complexes have gained increasing attention and become a research hotspot owing to their amazing structural geometries, rich properties as well as broad application value in the areas such as fluorescent probes, sensors, light-emitting materials, magnetic materials, electroluminescent devices, analysis test, cell imaging and so forth [1–4]. A lot of investigations on the lanthanide complexes have thus far been accomplished [5–9]. Multidentate ligands are often applied to prepare lanthanide complexes. As a multidentate ligand, 2,5-pyridinedicarboxylic acid ($2,5\text{-}H_2PA$) has several coordination sites (one nitrogen atom and four oxygen atoms) that allow it to coordinate to several lanthanide metal centers to build extended structures. Meanwhile, $2,5\text{-}H_2PA$ possesses a conjugated system which enables it to potentially exhibit photoluminescence. As a result, $2,5\text{-}H_2PA$ is a quite attractive synthon for designing and building novel lanthanide complexes with extended structures and interesting properties. Accordingly, we select $2,5\text{-}H_2PA$ to prepare lanthanide complexes that may have interesting structural motifs or properties. We report herein the preparation, characterization, photoluminescent and semiconductive properties of a novel lanthanide complex $[La(2,5\text{-}PA)(2,5\text{-}HPA)(H_2O)_2]_n \cdot nH_2O$ (**I**) with a two-dimensional (2D) layered structure. Complex **I** shows a photoluminescence emission in the green region of the light spectrum and a wide optical band gap of 3.57 eV.

EXPERIMENTAL

Materials and instrumentation. All chemicals of analytical reagent grade were commercially obtained and applied without further purification. Elemental analysis of carbon, hydrogen and nitrogen was performed with an Elementar Vario EL III microanalyser. Photoluminescence were measured with solid-state sample under room temperature on a F97XP spectrometer. Solid-state UV-Vis spectrum with powder samples was conducted at room temperature on a computer-controlled TU1901 UV/vis spectrometer equipped with an integrating sphere in the wavelength range of 190–900 nm. $BaSO_4$ powder was used as a 100% reflectance reference, on which the ground powder sample was coated.

Synthesis of complex I. It was prepared by mixing $La(NO_3)_3 \cdot 6H_2O$ (1 mmol, 433 mg), $2,5\text{-}H_2PA$

[1] The article is published in the original.

Table 1. Crystallographic data and structure refinements for complex **I**

Parameter	Value
M_r	524.17
Color/habit	Yellow/block
Crystal size, mm	0.15 × 0.11 × 0.09
Crystal system	Monoclinic
Space group	$P2_1/c$
a, Å	9.3068(7)
b, Å	19.1061(7)
c, Å	9.3292(3)
β, deg	101.735(4)
V, Å^3	1624.21(15)
Z	4
$2\theta_{max}$, deg	50
ρ_{calcd}, g/cm^3	2.144
μ/mm^{-1}	2.701
F(000)	1024
T/K	293(2)
Reflections collected	3332
Independent reflections (R_{int})	1616 (0.0296)
Observed reflections	1573
Parameters refined	253
Goodness-of-fit	1.009
R_1, wR_2	0.0318, 0.0698
Largest and mean Δ/σ	0.001 and 0
Δρ(max, min), e/Å^3	1.000, −0.709

(2 mmol, 334 mg) and 10 mL distilled water in a 25 mL Teflon-lined stainless steel autoclave and heated at 160°C for 10 days. After being slowly cooled down to room temperature at a rate of 6°C/h, yellow block crystals suitable for X-ray analysis were collected. The yield is 40% (based on La).

For $C_{14}H_{13}N_2O_{11}La$			
anal. calcd., %	C, 32.08	H, 2.50	N, 5.34
found, %	C, 31.99	H, 2.55	N, 5.26

X-ray structure determination. The intensity data were collected on a Rigaku Mercury CCD X-ray diffractometer with graphite monochromated MoK_α radiation (λ = 0.71073 Å) using a ω scan mode. CrystalClear software was applied for data reduction and empirical absorption corrections [10]. The structure was solved by the direct methods with the Siemens SHELXTL™ Version 5 package of crystallographic software [11]. The difference Fourier maps based on the atomic positions generated non-hydrogen atoms and the crystal structure was refined with a full-matrix least-squares refinement on F^2. All of the non-hydrogen atoms were refined anisotropically. Most of the hydrogen atoms were located theoretically and allowed to ride on the parent atoms, but those hydrogen atoms on the lattice water molecules were found by the difference Fourier maps. All the hydrogen atoms were included in the structural factor calculations with assigned isotropic thermal parameters but were not refined. Important crystallographic data and structural analyses are presented in Table 1, while the selected bond lengths and bond angles are depicted in Table 2.

Crystallographic data for the structural analysis have been deposited with the Cambridge Crystallographic Data Centre (CCDC no. 1570808; deposit@ccdc.cam.ac.uk or www:http://www.ccdc.cam.ac.uk).

RESULTS AND DISCUSSION

The single crystal X-ray diffraction analysis illustrates that complex **I** is comprised of neutral infinite 2D $[La(2,5\text{-PA})(2,5\text{-HPA})(H_2O)_2]_n$ layers and lattice water molecules. All of the crystallographic independent atoms are located at the general positions. The La^{3+} ion is surrounded by seven oxygen atoms and two nitrogen atoms from five 2,5-H_2PA ligands and two coordinating water molecules, yielding a slightly distorted monocapped square antiprism with the top and bottom planes defined by O(8) ($x-1$, y, z), O(5) ($-x$, $-y+1$, $-z+1$), O(2w), O(7) ($-x+1$, $-y+1$, $-z+2$) and O(1), O(5), N(2), N(1) atoms, respectively, as well as the O(1w) atom acting as the apex, as presented in Fig. 1. The bond length of La–N is 2.779(5) and 2.720(6) Å that is normal and comparable with those documented in the references [12–15]. The bond distance of La–$O_{2,5\text{-H2PA}}$ are in the span of 2.502(5)–2.627(4) Å with the average value being of 2.557(5) Å, which is close to that of La–O_{water} being of 2.597(5) and 2.531(5) Å, suggesting that 2,5-H2PA ligand and coordinating water molecules have similar attraction to the lanthanun ions. The bond angle of OLaO is in a wide range of 65.92(19)°–148.10(14)°. The bond angle of OLaN is also in a broad range of 59.23(14)°–147.19(17)°, while the bond angle of NLaN is 71.39(17)°.

In complex **I**, there are two kinds of crystallographic independent 2,5-H2PA ligands, namely, one of them acts as a terminal bidentate ligand chelating to a lanthanun ion with one nitrogen atom and one oxygen atom, while the other acts as a bridging quadridentate ligand coordinating to four lanthanun ions. The shortest distance between the neighboring La···La is 4.391(6) Å. The neighboring lanthanun ions are interconnected to each other through the quadridentate 2,5-H2PA ligand to construct an infinite 2D layer extending along the xz plane, as given in Fig. 2. There

Table 2. Selected bond lengths (Å) and bond angles (deg) for complex **I***

Bond	*d*, Å	Angle	ω, deg
La(1)–N(1)	2.779(5)	O(1)La(1)O(5)$^{\#3}$	79.2(1)
La(1)–N(2)	2.720(6)	O(1*w*)La(1)O(5)$^{\#3}$	78.5(1)
La(1)–O(1)	2.541(5)	O(8)$^{\#1}$La(1)O(5)	130.1(1)
La(1)–O(5)	2.627(4)	O(7)$^{\#2}$La(1)O(5)	135.3(2)
La(1)–O(8)$^{\#1}$	2.502(5)	O(2*w*)La(1)O(5)	71.8(2)
La(1)–O(7)$^{\#2}$	2.510(4)	O(1)La(1)O(5)	66.7(1)
La(1)–O(5)$^{\#3}$	2.607(4)	O(1*w*)La(1)O(5)	131.1(1)
La(1)–O(1*w*)	2.597(5)	O(5)$^{\#3}$La(1)O(5)	65.9(2)
La(1)–O(2*w*)	2.531(5)	O(8)$^{\#1}$La(1)N(2)	147.2(2)
Angle	ω, deg	O(7)$^{\#2}$La(1)N(2)	75.3(2)
O(8)$^{\#1}$La(1)O(7)$^{\#2}$	91.5(1)	O(2*w*)La(1)N(2)	72.8(2)
O(8)$^{\#1}$La(1)O(2*w*)	137.8(2)	O(1)La(1)N(2)	94.0 (2)
O(7)$^{\#2}$La(1)O(2*w*)	88.3(1)	O(1*w*)La(1)N(2)	127.0(2)
O(8)$^{\#1}$La(1)O(1)	70.4(1)	O(5)$^{\#3}$La(1)N(2)	124.2(2)
O(7)$^{\#2}$La(1)O(1)	128.0(1)	O(5)La(1)N(2)	60.8(2)
O(2*w*)La(1)O(1)	137.5(1)	O(8)$^{\#1}$La(1)N(1)	75.9(2)
O(8)$^{\#1}$La(1)O(1*w*)	72.7(2)	O(7)$^{\#2}$La(1)N(1)	69.3(1)
O(7)$^{\#2}$La(1)O(1*w*)	69.8(2)	O(2*w*)La(1)N(1)	141.5(2)
O(2*w*)La(1)O(1*w*)	67.8(2)	O(1)La(1)N(1)	59.2(1)
O(1)La(1)O(1*w*)	138.9(2)	O(1*w*)La(1)N(1)	126.7(1)
O(8)$^{\#1}$La(1)O(5)$^{\#3}$	82.3(2)	O(5)$^{\#3}$La(1)N(1)	137.5(2)
O(7)$^{\#2}$La(1)O(5)$^{\#3}$	148.1(1)	O(5)La(1)N(1)	102.0(1)
O(2*w*)La(1)O(5)$^{\#3}$	76.1(2)	N(2)La(1)N(1)	71.4(2)

* Symmetry codes: $^{\#1}$ $x-1, y, z$; $^{\#2}$ $-x+1, -y+1, -z+2$; $^{\#3}$ $-x, -y+1, -z+1$.

are some hydrogen-bonding interactions existing in complex **I**. All of the 2,5-H2PA ligands are involved in the formation of the hydrogen-bonding interactions. In complex **I**, there are totally two kinds of hydrogen-bonding interactions, i.e., O–H···O and C–H···O hydrogen-bonding interactions. The above-mentioned 2D layers and the lattice water molecules are interlinked via the hydrogen-bonding interactions to yield a 3D supramolecular network, as presented in Fig. 3. The result of the bond valence calculation verifies that the lanthanun ion is in +3 oxidation state (La(1): 3.14) [16]. To keep charge balance, the charge of 2,5-PA and 2,5-HPA must be −2 and −1, corresponding to the bridging quadridentate ligand and the terminal bidentate ligand, respectively. To the best of our knowledge, although a lot of lanthanide complexes containing 2,5-H2PA have thus far been reported [17–21], it is rare yet that a lanthanide complex containing both bidentate and quadridentate 2,5-H2PA ligands.

It is well known that lanthanide complexes can generally exhibit interesting photoluminescent behavior because they possess abundant *f*-orbital configurations. Meanwhile, lanthanide ions also possess attractive characteristics, i.e., they can show intensive photoluminescence and capability by tuning the photoluminescent emission region for specific applications in various wavelength ranges of the light spectrum. Furthermore, 2,5-H2PA-containing complexes are expected to display amazing photoluminescent properties because of the delocalized π-electrons of the pyridyl ring of the 2,5-H2PA. As a result, the title complex is supposed to exhibit photoluminescent properties. To confirm this and based on the above considerations, in the present work, we carried out the photoluminescent behaviors of complex **I** with powder samples at room temperature. The photoluminescent excitation and emission spectra of complex **I** are depicted in Fig. 4. The photoluminescent emission spectrum of complex **I** exhibits a narrow and strong emission band, while the photoluminescent excitation

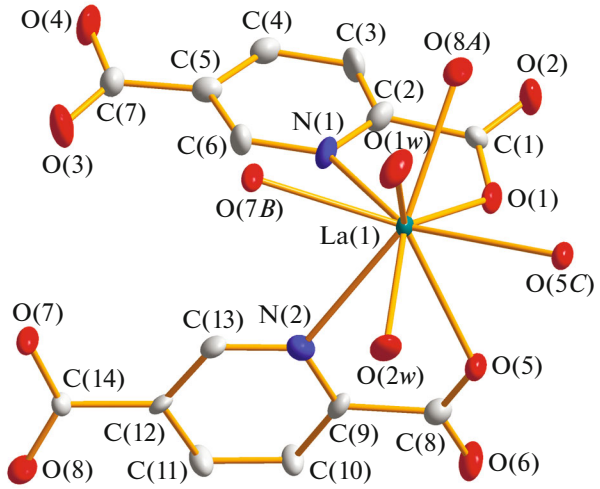

Fig. 1. An ORTEP drawing of complex **I** showing 50% thermal ellipsoids. Lattice water molecules and hydrogen atoms were omitted for clarity. Symmetry code: (*A*) $x - 1$, y, z; (*B*) $-x + 1$, $-y + 1$, $-z + 2$; (*C*) $-x$, $-y + 1$, $-z + 1$.

spectrum displays that the effective energy absorption is mainly located in the wavelength region of 300–340 nm. The photoluminescent excitation spectrum has a sharp band residing at 312 nm. When it was excited by the wavelength of 312 nm, the photoluminescent emission spectrum gives a narrow and intensive emission band at 481 nm in the green region of the light spectrum. As a result, complex **I** is probably a candidate for green photoluminescent materials.

The solid-state UV-Vis diffuse reflectance spectrum of complex **I** was recorded at room temperature with powder samples. After recording the diffuse reflectance spectra data set, it was dealt with the Kubelka–Munk function, i.e., $\alpha/S = (1 - R)^2/2R$. The parameter α is the absorption coefficient, S means the scattering coefficient which is practically wavelength independent if the particle diameter is larger than 5 μm, while R refers to the reflectance. The α/S vs. energy diagram is obtained based on the treatment of this function. The value of the energy band gap of complex **I** was determined by extrapolating from the linear portion of the absorption edges. The solid-state UV-Vis diffuse reflectance spectrum discovers that complex **I** exhibits a wide energy band gap of 3.57 eV, as shown in Fig. 5. As a result, complex **I** could be a potential material for wide band gap semiconductors. The slow slope of the energy absorption edge of complex **I** indicates that it might be an indirect transition [22]. The energy band gap of 3.57 eV of complex **I** is obviously larger than that of GaAs (1.4 eV), CdTe (1.5 eV) and $CuInS_2$ (1.55 eV), which are well-known for highly efficient photovoltaic compounds [23, 24].

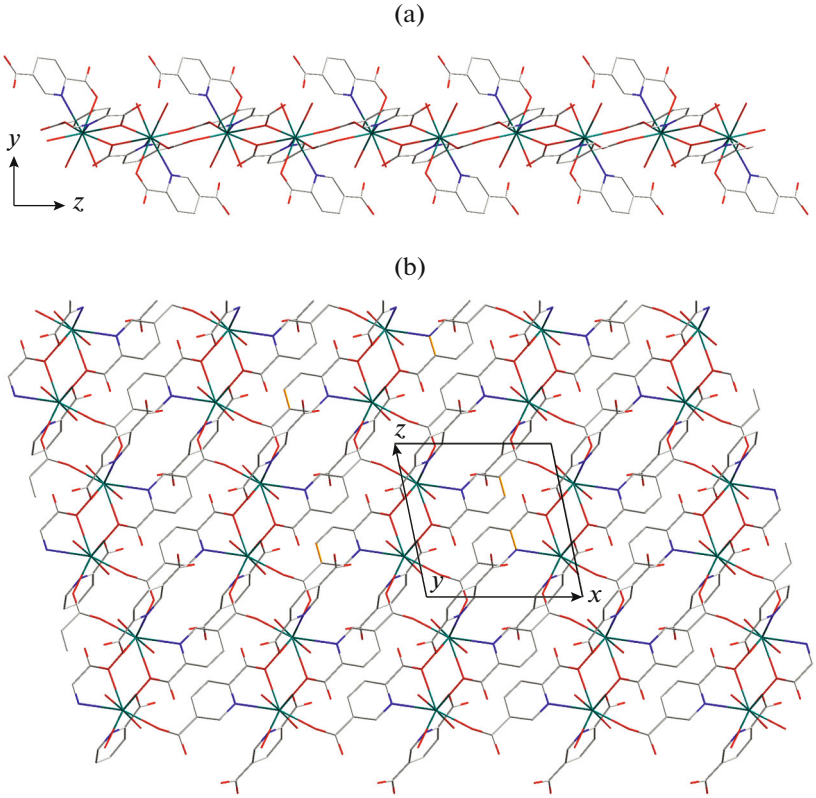

Fig. 2. The 2D layer of complex **I** viewed down along the *a* axis (a) and *b* axis (b).

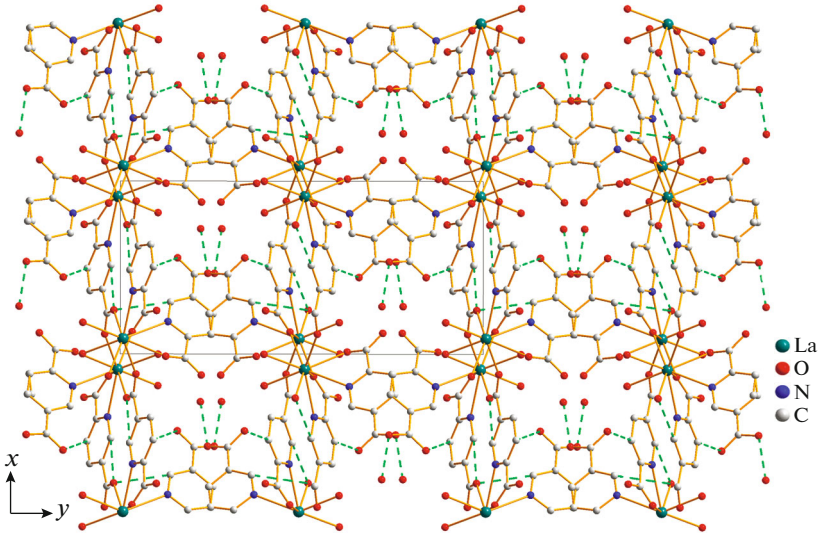

Fig. 3. Crystal packing diagram of complex **I** viewed down along the *c* axis. The dashed lines represent the hydrogen bonding interactions: O(4)–H(4*B*)···O(3*w*) 2.562(9) Å, 177°; C(6)–H(6*A*)···O(7) (1 – *x*, 1 – *y*, 2 – *z*) 3.018(9) Å, 116°; C(10)–H(10*A*)···O(3) (*x*, *y*, –1 + *z*) 3.509(8) Å, 167°; C(11)–H(11*A*)···O(1) (1 + *x*, *y*, *z*) 3.413(10) Å, 166°; C(13)–H(13*A*)···O(7) (1 – *x*, 1 – *y*, 2 – *z*) 3.118(9) Å, 127°.

In brief, we have prepared a novel lanthanide complex $[La(2,5\text{-}PA)(2,5\text{-}HPA)(H_2O)_2]_n \cdot nH_2O$ (**I**) through a hydrothermal reaction. Complex **I** is characteristic of a 2D layered structure with the La^{3+} ion possessing a slightly distorted monocapped square antiprism. The $[La(2,5\text{-}PA)(2,5\text{-}HPA)(H_2O)_2]_n$ layers and lattice water molecules interlink together through hydrogen bonding interactions to give a 3D supramolecular framework. Photoluminescence measurements with solid-state samples show that it displays an emission in the green region of the light spectrum. Solid-state UV-Vis spectrum reveals the existence of a wide optical band gap of 3.57 eV.

ACKNOWLEDGMENTS

We gratefully acknowledge the financial support of the NSF of China (no. 21361013) and the open foundation (no. 20150019) of the State Key Laboratory of Structural Chemistry, Fujian Institute of Research on the Structure of Matter, Chinese Academy of Sciences.

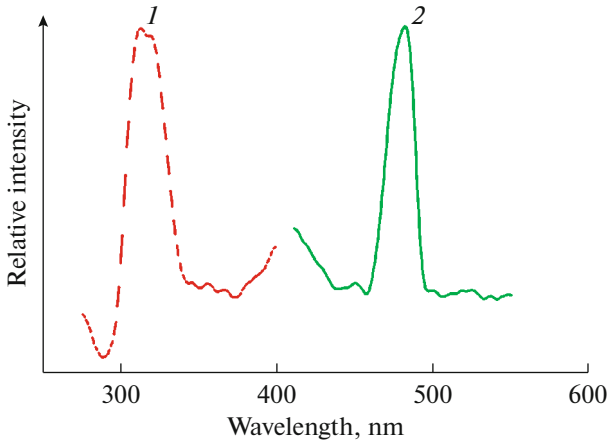

Fig. 4. The emission spectra of **I** measured with solid state sample under room temperature: excitation spectrum (*1*); emission spectrum (*2*).

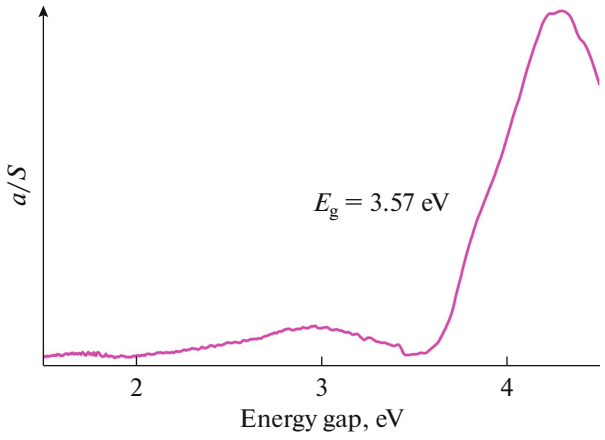

Fig. 5. Solid-state diffuse reflectance spectra for complex **I**.

REFERENCES

1. Goodwin, C.A.P., Ortu, F., Reta, D., et al., *Nature*, 2017, vol. 548, p. 439.
2. Adams, F., Machat, M.R., Altenbuchner, P.T., et al., *Inorg. Chem.*, 2017, vol. 56, p. 9754.
3. Massey, M., Medintz, I.L., Ancona, M.G., et al., *ACS Sensors*, 2017, vol. 2, p. 1205.
4. Welegedara, A.P., Yang, Y., Lee, M.D., et al., *Chem. Eur. J.*, 2017, vol. 23, p. 11694.
5. Creutz, S.E., Fainblat, R., Kim, Y., et al., *J. Am. Chem. Soc.*, 2017, vol. 139, p. 11814.
6. Lv, X.H., Yang, S.L., Li, Y.X., et al., *RSC Advances*, 2017, vol. 7, p. 38179.
7. Zhao, S., Hao, X.M., Liu, J.L., et al., *J. Solid State Chem.*, 2017, vol. 255, p. 76.
8. Doessing, A., Kadziola, A., Gawryszewska, P., et al., *Inorg. Chim. Acta*, 2017, vol. 467, p. 93.
9. Griffiths, K., Tsipis, A.C., Kumar, P., et al., *Inorg. Chem.*, 2017, vol. 56, p. 9563.
10. Rigaku, *CrystalClear, Version 1.35*, Tokyo (Japan): Rigaku Corp., 2002.
11. Siemens, *SHELXTL^{TM}, Version 5, Reference Manual*, Madison: Siemens Energy & Automation Inc., 1994.
12. Bag, P., Maji, S.K., Biswas, P., et al., *Polyhedron*, 2013, vol. 52, p. 976.
13. Holynska, M. and Korabik, M., *Eur. J. Inorg. Chem.*, 2013, vol. 54, p. 69.
14. Fang, W.-H., Cheng, L., Huang, L., et al., *Inorg. Chem.*, 2013, vol. 52, p. 6.
15. Cole, M.L., Deacon, G.B., Forsyth, C.M., et al., *Chem. Eur. J.*, 2013, vol. 19, p. 1410.
16. O'Keeffe, M. and Brese, N.E., *J. Am. Chem. Soc.*, 1991, vol. 113, p. 3226.
17. Ji, B., Deng, D., He, X., et al., *Inorg. Chem.*, 2012, vol. 51, p. 2170.
18. Silva, P., Cunha-Silva, L., Silva, N.J.O., et al., *Cryst. Growth Des.*, 2013, vol. 13, p. 2607.
19. Yang, A.H., Gao, H.L., Cui, J.Z., et al., *CrystEng-Comm*, 2011, vol. 13, p. 1870.
20. Shi, L.X., Xu, X., and Wu, C.D., *CrystEngComm*, 2011, vol. 13, p. 6027.
21. Wu, M., Jiang, F., Zhou, Y., et al., *Inorg. Chem. Commun.*, 2012, vol. 15, p. 25.
22. Huang, F.Q., Mitchell, K., and Ibers, J.A., *Inorg. Chem.*, 2001, vol. 40, p. 5123.
23. Dürichen, P. and Bensch, W., *Eur. J. Solid State Inorg. Chem.*, 1997, vol. 34, p. 1187.
24. Tillinski, R., Rumpf, C., Nather, C., et al., *Z. Anorg. Allg. Chem.*, 1998, vol. 624, p. 1285.